



Aalborg Universitet

**AALBORG UNIVERSITY**  
DENMARK

## **A New Three-Phase Multi-Level Asymmetrical Inverter With Optimum Hardware Components**

Chittathuru, Dhanamjayulu; Kaliannan, Palanisamy; Padmanaban, Sanjeevikumar; Maroti, Pandav Kiran; Holm-Nielsen, Jens Bo

*Published in:*  
IEEE Access

*DOI (link to publication from Publisher):*  
[10.1109/ACCESS.2020.3039831](https://doi.org/10.1109/ACCESS.2020.3039831)

*Creative Commons License*  
CC BY 4.0

*Publication date:*  
2020

*Document Version*  
Publisher's PDF, also known as Version of record

[Link to publication from Aalborg University](#)

*Citation for published version (APA):*

Chittathuru, D., Kaliannan, P., Padmanaban, S., Maroti, P. K., & Holm-Nielsen, J. B. (2020). A New Three-Phase Multi-Level Asymmetrical Inverter With Optimum Hardware Components. *IEEE Access*, 8, 212515-212528. <https://doi.org/10.1109/ACCESS.2020.3039831>

### **General rights**

Copyright and moral rights for the publications made accessible in the public portal are retained by the authors and/or other copyright owners and it is a condition of accessing publications that users recognise and abide by the legal requirements associated with these rights.

- Users may download and print one copy of any publication from the public portal for the purpose of private study or research.
- You may not further distribute the material or use it for any profit-making activity or commercial gain
- You may freely distribute the URL identifying the publication in the public portal -

### **Take down policy**

If you believe that this document breaches copyright please contact us at [vbn@aub.aau.dk](mailto:vbn@aub.aau.dk) providing details, and we will remove access to the work immediately and investigate your claim.

Received November 1, 2020, accepted November 17, 2020, date of publication November 24, 2020, date of current version December 9, 2020.

Digital Object Identifier 10.1109/ACCESS.2020.3039831

# A New Three-Phase Multi-Level Asymmetrical Inverter With Optimum Hardware Components

C. DHANAMJAYULU<sup>1,2</sup>, (Member, IEEE),  
PALANISAMY KALIANNAN<sup>1,2</sup>, (Senior Member, IEEE),  
SANJEEVIKUMAR PADMANABAN<sup>2</sup>, (Senior Member, IEEE),  
PANDAV KIRAN MAROTI<sup>2</sup>, (Member, IEEE),  
AND JENS BO HOLM-NIELSEN<sup>2</sup>, (Senior Member, IEEE)

<sup>1</sup>School of Electrical Engineering, Vellore Institute of Technology, Vellore 632014, India

<sup>2</sup>Department of Energy Technology, Aalborg University, 6700 Esbjerg, Denmark

Corresponding authors: C. Dhanamjayulu (dhanamjayulu.c@vit.ac.in) and Sanjeevikumar Padmanaban (san@et.aau.dk)

This work was supported by the Ministry of Foreign Affairs of Denmark (MFA), Act 7 on Denmark's International Development Cooperation, Danida Mobility Grant, under Project 19-MG06AAU.

**ABSTRACT** In this article, a novel three-phase asymmetrical multilevel inverter is presented. The proposed inverter is designed with an optimal hardware components to generate three-phase nineteen output voltage levels. The proposed inverter exhibits various advantages like a suitable output voltage waveform with improved power quality, lower total harmonic distortion (THD), and more moderate complexity, reduction in cost, reduced power losses, and improved efficiency. A comparison of the proposed topology in terms of several parameters with existing methods illustrates its merits and features. The proposed inverter tested with steady-state and dynamic load disturbances. Various experimental results are included in this article to validate the performance of the proposed inverter during various extremities. In addition, a detailed comparison is tabulated between simulation and experimental results graphically. The proposed inverter has been stable even during load disturbance conditions. The simulation and feasibility model are verified using a prototype model.

**INDEX TERMS** Multilevel inverter (MLI), total harmonic distortion, asymmetrical multilevel inverter.

## I. INTRODUCTION

The multilevel inverter is gaining a lot of importance in industrial and high-power applications because of the usage of low-level inverter results in an output with more significant harmonics. So, the research and study of these multilevel inverters are gaining a lot of importance. There are different methods to realize the working of multilevel inverters [1]–[6]. The most prominent among these topologies is neutral point clamped inverters, the flying capacitors, and the cascaded inverters [2]. These topologies are aided with different switching patterns like single pulse width modulation SPWM, multi-carrier pulse width modulation MCPWM, and staircase modulation technique to achieve AC output voltage waveform with lower harmonics. With an increased number of levels of the inverter, the THD improves. In a neutral point clamped method [7]–[9], diodes are used to facilitate multiple voltage levels to the capacitor bank connected in cascade

mode via various phases. The diodes are the clamping devices that allow limited voltage to transfer through them, reducing the stress from other devices. The peak voltage of these inverters is half of the energy supplied, which is one shortfall and the same can be eliminated by aggregating the number of diodes, switches, and condensers, the output voltage is limited and for over three-levels the charge balance gets disturbed. The applications of these inverters include static Var compensation, variable motor speed drives, high voltage DC and AC transmission lines, high voltage system interconnection. Flying capacitors [10] topology is quite similar to the diode-clamped multilevel inverter, but capacitors clamping devices in this method, unlike the diode-clamped MLI [23]–[39].

In recent past, modular multilevel converters (MMC) are suited for high-voltage applications and these are introduced with various sub-modules, where each sub-module comprises two switches with a DC capacitor. The switching losses and harmonics are less. Number of switches and capacitors are used in this topology, which increases the control complexity

The associate editor coordinating the review of this manuscript and approving it for publication was Atif Iqbal<sup>1</sup>.

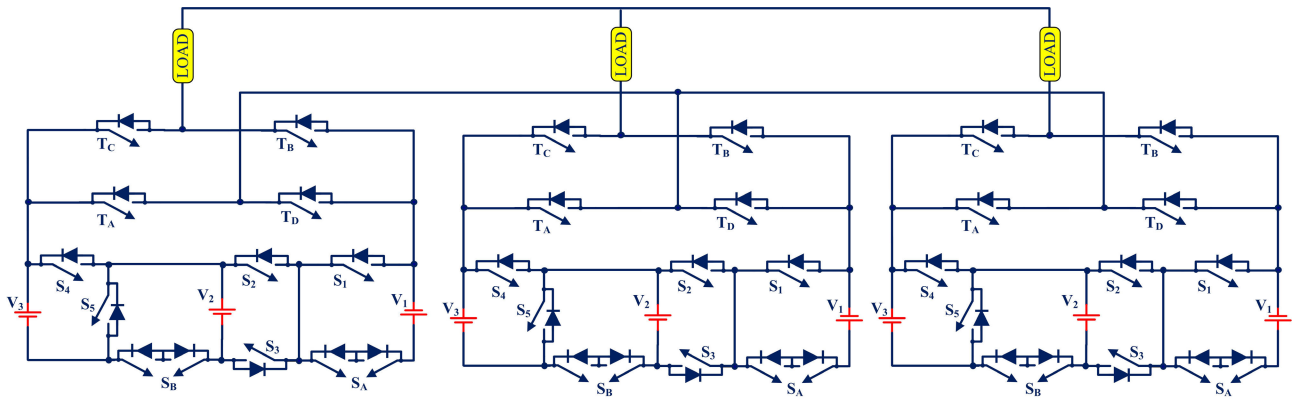


FIGURE 1. Proposed Three-Phase Configuration of 19MLI.

and cost [11], [12]. There are three types of multilevel inverters neutral point clamped (NPC) [13], Cascade H-bridge inverter (CHB) [14] and flying capacitor (FC) [15]. Number of switches and clamping diodes are used in diode-clamped inverter for higher levels, moreover the balancing of capacitors is a challenging task as these are connected in series. Even for higher levels, larger number of capacitors are used in flying capacitor where the balancing of voltage is complex [16].

The advantage of symmetric structures is modularity that can able to design and extend easily. Two such inverter structures are presented in [17], [18], where the mixture of basic units and H-bridge used based on non-isolated DC sources require number of switches, increases the control complexity, size and cost. A new multilevel inverter topology with insulated driver circuit and reduced number of switches has been presented in [19]. In addition, the calculation of DC voltage sources is proposed, and it comprises four high rating switches. This requires a bi-directional switch for the blocking voltage and conducting current in both directions.

In [20], a three-phase multilevel inverter suited for electrical drive applications has been presented. Counterpart of the CHB inverters, power cells are cascaded, and each cell is having two series legs. The design equations for the load voltage with steps carried out using pulse-width modulation phase shifting multi-carrier modulation technique are analyzed. There are several DC voltage sources in this topology results in the increase in the total cost of the inverter which is a disadvantage of this structure.

A new topology of multilevel inverter is presented in [21]. This structure mainly focuses on reducing the power transistors regarding the number of levels. Various equations are derived mathematically. This requires a bi-directional switch for the blocking voltage and conducting current in both directions.

This article presents a reduced circuit part for renewable energy applications, counting inverter topology at nineteen levels. This manuscript presents a 19-level asymmetric cascaded MLI with reduced DC sources and switches with relatively low THD. The proposed inverter is implemented

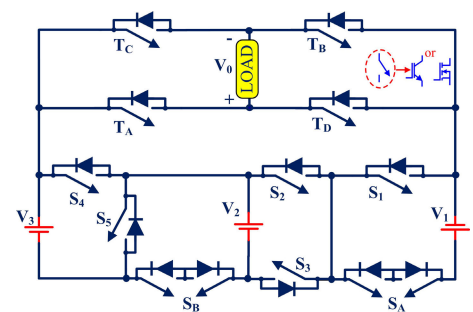


FIGURE 2. Proposed Phase Leg-A Configuration of 19MLI.

and tested only with a resistive, inductive load, and dynamic variations in the load from R to L and vice versa. The analysis of total standing voltage can be done [22]. During the dynamic load period conditions, the proposed inverter is well stabilized [23]–[41], and this inverter is suitable for renewable energy applications [23]–[41].

The article was structured as follows. Section II that follows contains the details of the proposed topology of 19-levels. Part III presents the parameter calculations, section IV presents the loss and efficiency, section V presents TSV calculation, and section VI and section VII present the findings of the analysis and experiment along with the simulation results.

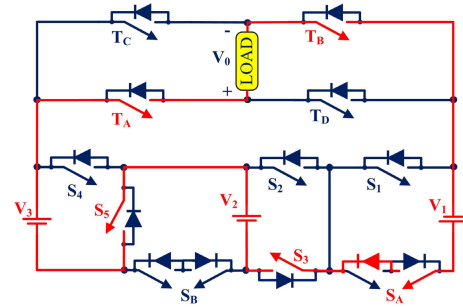
## II. PROPOSED THREE-PHASE ASYMMETRICAL INVERTER TOPOLOGY

The proposed three-phase 19-level-inverter is shown in Fig.1. The topology proposed for each phase comprises two bidirectional and nine unidirectional power semiconductor switches for each phase leg is shown in Fig.2. The bidirectional switches are used to avoid short-circuits and to block currents in both directions for the DC supply. In this topology, usually, the desired voltage is realized from different DC voltage links or sources. Based on the DC sources, the cascaded MLIs are classified as symmetrical(equal) and asymmetrical(unequal) inverters. In symmetrical type, the voltage of the DC links is held at the same level. The demerit of symmetrical topology is that with the increase in output voltage levels, the number of switches also increases. In order to overcome this,

**TABLE 1.** Conduction states of switches.

L	S <sub>1</sub>	S <sub>2</sub>	S <sub>3</sub>	S <sub>4</sub>	S <sub>5</sub>	S <sub>A</sub>	S <sub>B</sub>	T <sub>A</sub>	T <sub>B</sub>	T <sub>C</sub>	T <sub>D</sub>	V <sub>O</sub> (V)
1	0	0	1	0	1	1	0	1	1	0	0	V <sub>1</sub> +V <sub>2</sub> +V <sub>3</sub> =400.5
2	0	1	0	0	1	1	0	1	1	0	0	V <sub>1</sub> +V <sub>3</sub> =356
3	0	1	0	0	0	1	1	1	1	0	0	V <sub>1</sub> -V <sub>2</sub> +V <sub>3</sub> =311.5
4	1	0	1	0	1	0	0	1	1	0	0	V <sub>2</sub> +V <sub>3</sub> =267
5	1	1	0	0	1	0	0	1	1	0	0	V <sub>3</sub> =222.5
6	0	0	1	1	0	1	0	1	1	0	0	V <sub>1</sub> +V <sub>2</sub> =178
7	0	1	0	1	0	1	0	1	1	0	0	V <sub>1</sub> =133.5
8	0	1	0	1	1	1	1	1	1	0	0	V <sub>1</sub> -V <sub>2</sub> =89
9	1	0	1	1	0	0	0	1	1	0	0	V <sub>2</sub> =44.5
10	0	0	0	0	0	0	0	1	1	0	0	0V
11	1	0	1	1	0	0	0	0	0	1	1	-V <sub>2</sub> =-44.5
12	0	1	0	1	1	1	1	0	0	1	1	-(V <sub>1</sub> -V <sub>2</sub> )=-89
13	0	1	0	1	0	1	0	0	0	1	1	-V <sub>1</sub> =-133.5
14	0	0	1	1	0	1	0	0	0	1	1	-(V <sub>1</sub> +V <sub>2</sub> )=-178
15	1	1	0	0	1	0	0	0	0	1	1	-V <sub>3</sub> =-222.5
16	1	0	1	0	1	0	0	0	0	1	1	-(V <sub>2</sub> +V <sub>3</sub> )=-267
17	0	1	0	0	0	1	1	0	0	1	1	-(V <sub>1</sub> -V <sub>2</sub> +V <sub>3</sub> )=-311.5
18	0	1	0	0	1	1	0	0	0	1	1	-(V <sub>2</sub> +V <sub>3</sub> )=-356
19	0	0	1	0	1	1	0	0	0	1	1	-(V <sub>1</sub> +V <sub>2</sub> +V <sub>3</sub> )=-400.5

the DC links are supplied with unequal voltages called the asymmetrical topology. In the proposed 19 level asymmetrical MLI, the switches are selected based on the strategy in avoiding short circuit in the specified path of current traversal. The initial level is got by conducting the switches S<sub>3</sub>, S<sub>5</sub>, S<sub>A</sub>, T<sub>A</sub> and T<sub>B</sub> forming a closed path precisely without short circuit. In this mode of operation, the blocking voltage of switches is in calculating the total standing voltage. In the second mode of operation, the switches S<sub>2</sub>, S<sub>5</sub>, S<sub>A</sub>, T<sub>A</sub>, T<sub>B</sub> are in conduction. These are selected for avoiding the short circuit, and even the addition of maximum blocking voltages of each semiconductor switch is lesser in value, which results in less TSV and cost effective. Similarly, the switch selection patterns up to 19 level are represented in Table.3. Based on this look-up table, the switches are selected based on the above conditions in which the overall loop of conduction of switches provides an efficient operation of an inverter with less standing voltage across switches. The proposed topology is implemented with three unequal DC sources namely, V<sub>1</sub>=133.5, V<sub>2</sub>=44.5V, and V<sub>3</sub>=222.5V and load resistance 100 ohms, respectively. The switching losses in the system depend on switching frequency, which is less because of the reduced voltage. This topology also comprises the combining of various switches to enhance the efficiency of the inverter. The switching states for the proposed inverter are tabulated in Table 1. The proposed inverter phase A and modes of operation are shown in Fig.3 to 21, respectively. In Mode-1, the power switches S<sub>3</sub>, S<sub>5</sub>, S<sub>A</sub>, T<sub>A</sub>, and T<sub>B</sub> are turn-on(conduction state) and remaining switches will turn-off then, the output voltage is the sum of V<sub>O</sub>=V<sub>1</sub> + V<sub>2</sub> + V<sub>3</sub>=+400.5V at the load ends. In Mode-2, the power switches S<sub>2</sub>, S<sub>5</sub>, S<sub>A</sub>, T<sub>A</sub>, and T<sub>B</sub> are turn-on(conduction state) and remaining switches will turn-off then, the output voltage is the sum of V<sub>O</sub>=V<sub>1</sub>+V<sub>3</sub> = +356V at the load ends. In Mode-3, the power switches S<sub>2</sub>, S<sub>A</sub>, S<sub>B</sub>, T<sub>A</sub>, and T<sub>B</sub> are turn-on(conduction state) and remaining switches will turn-off then, the output voltage is the sum of V<sub>O</sub>=V<sub>1</sub>-V<sub>2</sub>+V<sub>3</sub> = +311.5V at the load ends.

**FIGURE 3.** Mode-1  $V_O = V_1 + V_2 + V_3 = +400.5V$ .

In Mode-4, the power switches S<sub>1</sub>, S<sub>3</sub>, S<sub>5</sub>, T<sub>A</sub>, and T<sub>B</sub> are turn-on(conduction state) and remaining switches will turn-off then, the output voltage is the sum of V<sub>O</sub>=V<sub>2</sub>+V<sub>3</sub> = +267V at the load ends. In Mode-5, the power switches S<sub>1</sub>, S<sub>2</sub>, S<sub>5</sub>, T<sub>A</sub>, and T<sub>B</sub> are turn-on(conduction state) and remaining switches will turn-off then, the output voltage is V<sub>O</sub>=V<sub>3</sub> = +222.5V at the load ends. In Mode-6, the power switches S<sub>3</sub>, S<sub>4</sub>, S<sub>A</sub>, T<sub>A</sub>, and T<sub>B</sub> are turn-on(conduction state) and remaining switches will turn-off then, the output voltage is the sum of V<sub>O</sub>=V<sub>1</sub>+V<sub>2</sub> = +178V at the load ends. In Mode-7, the power switches S<sub>2</sub>, S<sub>4</sub>, S<sub>A</sub>, T<sub>A</sub>, and T<sub>B</sub> are turn-on(conduction state) and remaining switches will turn-off then, the output voltage is V<sub>O</sub>=V<sub>1</sub>=+133.5V at the load ends. In Mode-8, the power switches S<sub>2</sub>, S<sub>4</sub>, S<sub>5</sub>, S<sub>A</sub>, S<sub>B</sub>, T<sub>A</sub>, and T<sub>B</sub> are turn-on(conduction state) and remaining switches will turn-off then, the output voltage is the sum of V<sub>O</sub>=V<sub>1</sub>-V<sub>2</sub>=89V at the load ends. In Mode-9, the power switches S<sub>1</sub>, S<sub>3</sub>, S<sub>4</sub>, T<sub>A</sub>, and T<sub>B</sub> are turn-on (conduction state) and remaining switches will turn-off then, the output voltage is V<sub>O</sub>=V<sub>2</sub>=44.5V at the load ends. In Mode-10, the power switches T<sub>B</sub>, and T<sub>D</sub> are turn-on(conduction state) and remaining switches will turn-off then, the output voltage is V<sub>O</sub>=0V at the load ends. In Mode-11, the power switches S<sub>1</sub>, S<sub>3</sub>, S<sub>4</sub>, T<sub>C</sub>, and T<sub>D</sub> are turn-on(conduction state) and remaining switches will turn-off then, the output voltage is V<sub>O</sub> = -V<sub>2</sub> = -44.5V at the load ends. In Mode-12, the power switches S<sub>2</sub>, S<sub>4</sub>, S<sub>5</sub>, S<sub>A</sub>, S<sub>B</sub>, T<sub>C</sub>, and T<sub>D</sub> are turn-on(conduction state) and remaining switches will turn-off then, the output voltage is the sum of V<sub>O</sub> = -(V<sub>1</sub>-V<sub>2</sub>) = -89V at the load ends. In Mode-13, the power switches S<sub>2</sub>, S<sub>4</sub>, S<sub>A</sub>, T<sub>C</sub>, and T<sub>D</sub> are turn-on(conduction state) and remaining switches will turn-off then, the output voltage is V<sub>O</sub> = -V<sub>1</sub> = -133.5V at the load ends. In Mode-14, the power switches S<sub>3</sub>, S<sub>4</sub>, S<sub>A</sub>, T<sub>C</sub>, and T<sub>D</sub> are turn-on(conduction state) and remaining switches will turn-off then, the output voltage is the sum of V<sub>O</sub> = -(V<sub>1</sub> + V<sub>2</sub>) = -178V at the load ends. In Mode-15, the power switches S<sub>1</sub>, S<sub>2</sub>, S<sub>5</sub>, T<sub>C</sub>, and T<sub>D</sub> are turn-on(conduction state) and remaining switches will turn-off then, the output voltage is V<sub>O</sub> = -V<sub>3</sub> = -222.5V at the load ends. In Mode-16, the power switches S<sub>1</sub>, S<sub>3</sub>, S<sub>5</sub>, T<sub>C</sub>, and T<sub>D</sub> are turn-on(conduction state) and remaining switches will turn-off then, the output voltage is the sum of V<sub>O</sub> = -(V<sub>2</sub> + V<sub>3</sub>) = -267V at the load ends. In Mode-17, the power switches S<sub>2</sub>, S<sub>A</sub>, S<sub>B</sub>, T<sub>C</sub>, and



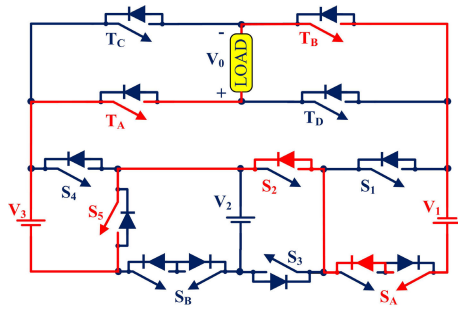


FIGURE 4. Mode-2  $V_O = V_1 + V_3 = +356V$ .

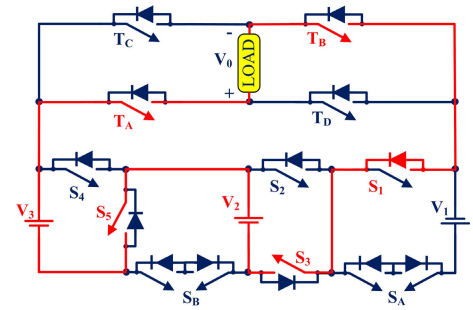


FIGURE 6. Mode-4  $V_O = V_2 + V_3 = +267V$ .

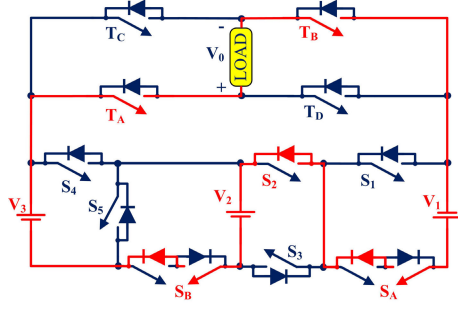


FIGURE 5. Mode-3  $V_O = V_1 - V_2 + V_3 = +311.5V$ .

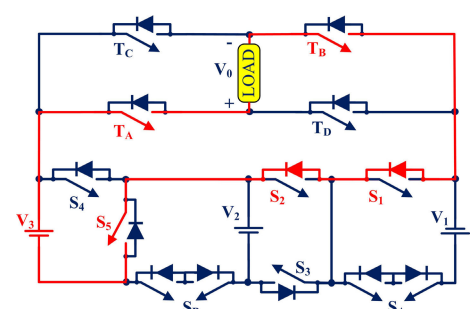


FIGURE 7. Mode-5  $V_O = V_3 = +222.5V$ .

$T_D$  are turn-on(conduction state) and remaining switches will turn-off then, the output voltage is the sum of  $V_O = -(V_1 - V_2 + V_3) = -311.5V$  at the load ends. In Mode-18, the power switches  $S_2, S_5, S_A, T_C$ , and  $T_D$  are turn-on(conduction state) and remaining switches will turn-off then, the output voltage is the sum of  $V_O = -(V_1 + V_3) = -356V$  at the load ends. In Mode-19, the power switches  $S_3, S_5, S_A, T_C$ , and  $T_D$  are turn-on(conduction state) and remaining switches will turn-off then, the output voltage is the sum of  $V_O = -(V_1 + V_2 + V_3) = -400.5V$  at the load ends. The expected (typical) output and gate pulse waveform are shown in Fig.22 and simulation output voltage, current, THD, and gate pulses are generated by staircase pulse width modulation technique are shown in Fig.23 to Fig.27 respectively. The proposed 19 level asymmetrical MLI is designed in such a way that the desired output voltage to be 400V. This can be achieved by the proper design of DC sources, such as  $V_1=133.5V$ ,  $V_2=44.5V$  and  $V_3=222.5V$  based on the number of levels and proposed topology. The selection of bidirectional switches at a specific location avoids the short circuit and blocks the current in both directions for a DC supply. The selected DC sources are tested with various modes of operation based on the conduction of switches regarding the switching frequency, and the expected output is achieved, which is explained in Table.1.

#### A. DEVELOPMENT OF POTENTIAL MLI PARAMETERS

Parameters for the proposed topology circuit are set as:

The switches number(No. of switches) are calculated as;

$$N_{switches} = 3k + 2 \quad (1)$$

If  $k$  is the no. of sources, then the switches no. of switches =  $3 * 3 + 4 = 13$  by taking  $k=3$ .

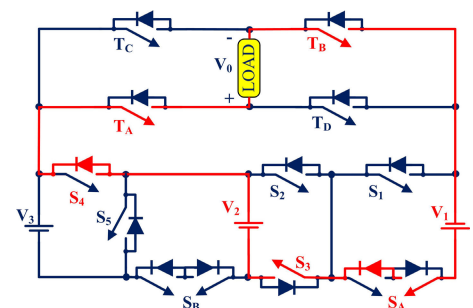


FIGURE 8. Mode-6  $V_O = V_1 + V_2 = +178V$ .

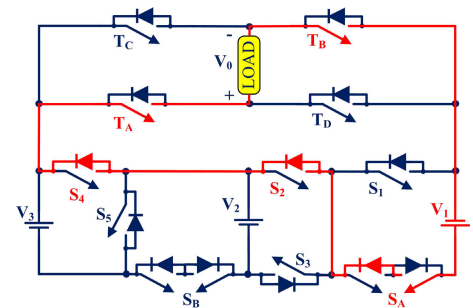


FIGURE 9. Mode-7  $V_O = V_1 = +133.5V$ .

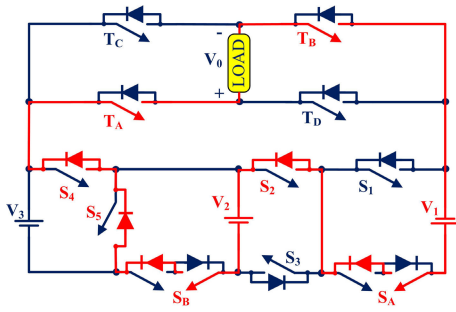
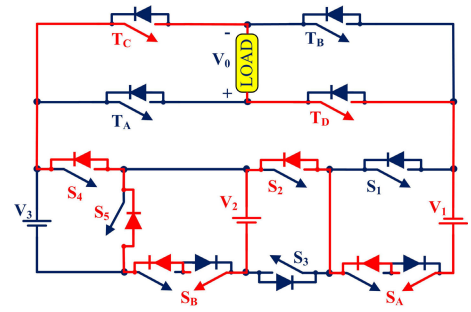
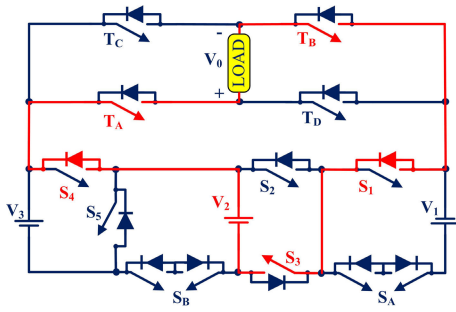
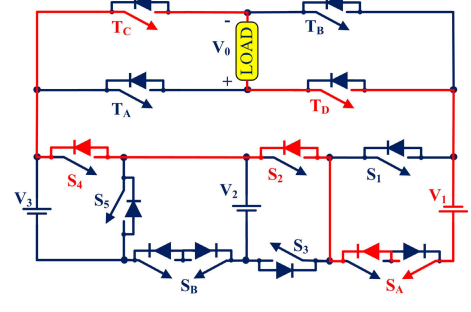
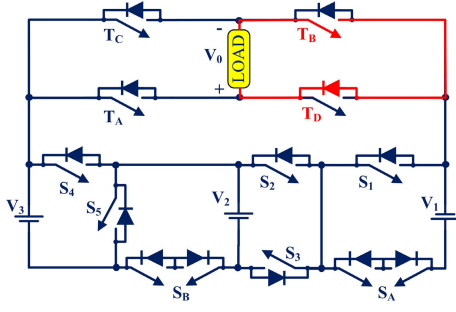
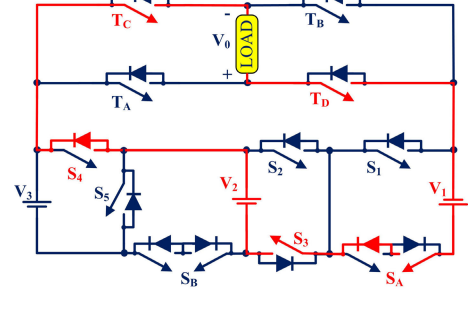
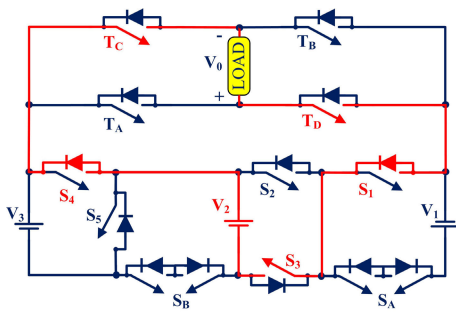
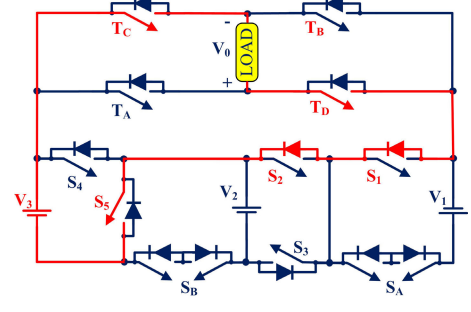
The sources no. of are calculated as:

$$N_{source} = k \quad (2)$$

Then the sources are  $N_{source}=3$ , taking  $k=3$

The output level No. of is got as;

$$N_{levels} = 2 \left( 2^k \right) + 3 \quad (3)$$

FIGURE 10. Mode-8  $V_0 = V_1 - V_2 = 89V$ .FIGURE 14. Mode-12  $V_0 = -(V_1 - V_2) = -89V$ .FIGURE 11. Mode-9  $V_0 = V_2 = 44.5V$ .FIGURE 15. Mode-13  $V_0 = -V_1 = -133.5V$ .FIGURE 12. Mode-10  $V_0 = 0V$ .FIGURE 16. Mode-14  $V_0 = -(V_1 + V_2) = -178V$ .FIGURE 13. Mode-11  $V_0 = -V_2 = -44.5V$ .FIGURE 17. Mode-15  $V_0 = -V_3 = -222.5V$ .

Then the level no. of is  $N_{level} = 2(2^3 + 3) = 19$  with  $k=3$   
The voltage from the output is defined as;

$$V_{output} = \left[ \left( 2^k \right) + 1 \right] * V_2 \quad (4)$$

Then the voltage of the output is  
 $V_{output} = (2^3 + 1) * 44.5 = 400.5V$ , taking  $k=3$  and  $V_2 = V_{dc} = 44.5V$ .

### III. POWER LOSS AND EFFICIENCY CALCULATION OF MLI

The losses can be calculated in both cases, the losses of conduction and losing switching are the two key losses that follow switches. The conduction losses can be got as follows;

$$P_{CI\_IGBT(t)} = [V_{IGBT} + R_{IGBT} i^\alpha(t)] i(t) \quad (5)$$

where  $V_{IGBT}$  is IGBT forward voltage drop, and  $V_{d}$  is diode drop forward voltage. The  $\alpha$  is a constant for the

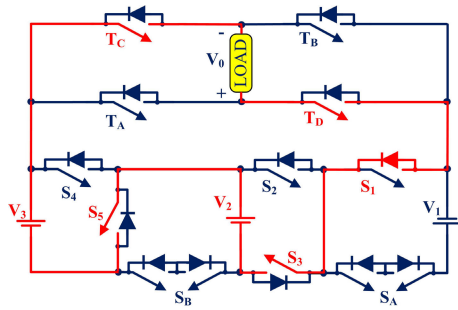


FIGURE 18. Mode-16  $V_0 = -(V_2 + V_3) = -267V$ .

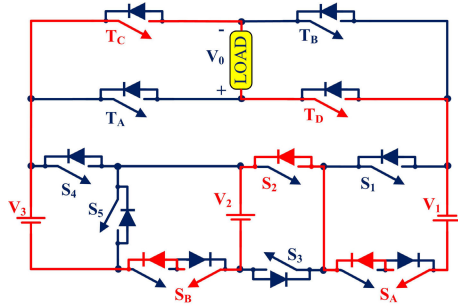


FIGURE 19. Mode-17  $V_0 = -(V_1 - V_2 + V_3) = -311.5V$ .

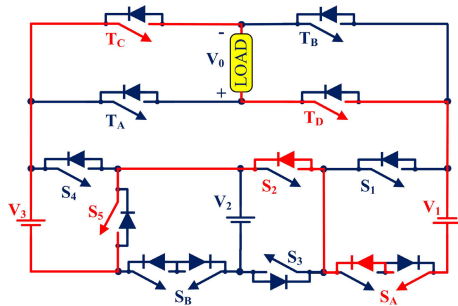


FIGURE 20. Mode-18  $V_0 = -(V_1 + V_3) = -356V$ .

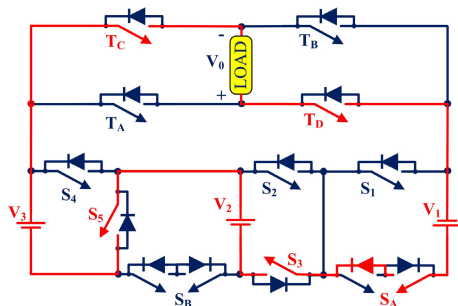


FIGURE 21. Mode-19  $V_0 = -(V_1 + V_2 + V_3) = -400.5V$ .

IGBT specification [41], [42], and  $R_{IGBT}$  is the equivalent resistance of the IGBTs and  $R_d$  is the equivalent resistance of the diodes [41], [42]. The average value of the conductive power loss ( $P_{cl}$ ) of the multilevel inverter can be given as follows [41], [42], considering that the current path includes both  $N_{IGBT}$  transistor and  $N_d$  diodes at the moment  $t$  [47].

$$P_{Cl} = \frac{1}{2\pi} \int_0^{2\pi} [N_{IGBT}(t) P_{cl,IGBT}(t) dt] \quad (6)$$

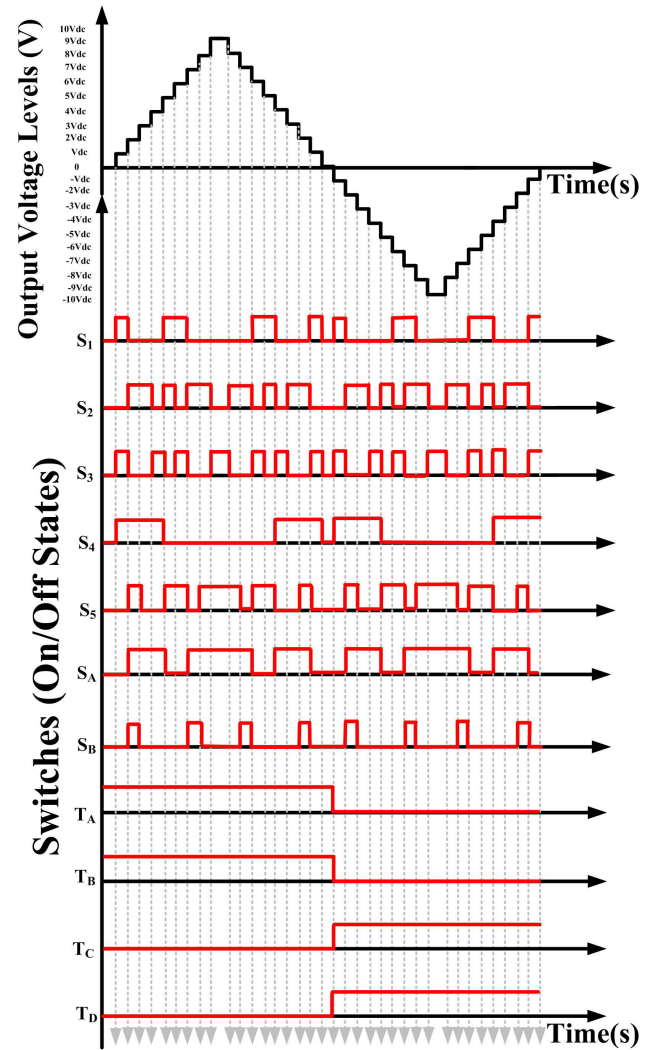


FIGURE 22. Expected (Typical) Output and Gate pulse waveform of 19 MLI.

Switching loss can be calculated according to the capacity used in the switches. Losses may be got depending on the turn-on and turn-off times of the switches. The losses from switching can be estimated based on linear differences in switching current and voltage. The energy figures are: Where  $En_{on}$  and  $En_{off}$  are respectively the witch  $k$  turn-ON and turn-OFF losses. The losses from switching are equal to the sum of power losses from turn-on and turn-off, calculated:

$$P_{Sl} = f \sum_{K=1}^{N_{switch}} \left[ \sum_{j=1}^{N_{on,k}} En_{on,kj} + \sum_{j=1}^{N_{off,k}} En_{off,kj} \right] \quad (7)$$

The total power losses calculated as follows ( $P_{total loss}$ )

$$P_{total loss} = P_{cl} + P_{sl} \quad (8)$$

The efficiency of the Inverter given below

$$Efficiency = \frac{P_{out}}{P_{in}} = \frac{P_{out}}{P_{out} + P_{loss}} \quad (9)$$

where the output power and the input power are  $P_{out}$  and  $P_{in}$ , respectively.

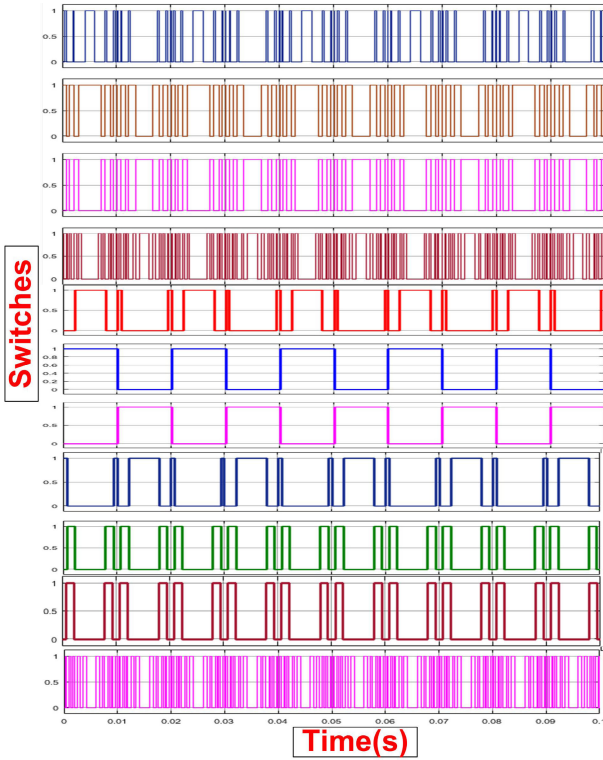


FIGURE 23. Simulation Gate pulse waveforms of 19 MLI.

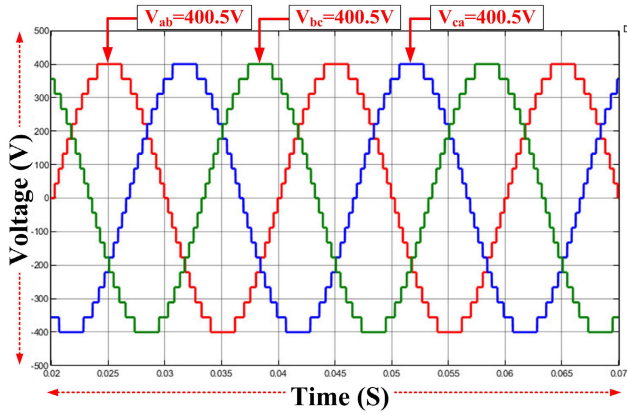


FIGURE 24. Simulation Three-Phase output waveform of 19 MLI.

Can estimate the output power as follows;

$$P_{out} = V_{rms} * I_{rms} \quad (10)$$

Using equation (10) ( $V_{rms} = 282.4V$  &  $I_{rms} = 2.828A$ ) the experimental output power of 799.87 W is got. For measurement, the parameter values are taken from the IGBT CM75DU-12 datasheet [41], [42]. The  $V_{switch}$  value (0.6V) is taken from the plot of performance characteristics and RIGBT is 0.4-ohm, turn-on delay as 100 ns, turn-on up time as 250 ns, turn off delay time as 200 ns and turn off fall time as 300 ns for 11 switches [41], [42]. The proposed inverter architecture would require 37 measures in one full cycle. The conduction losses are determined by using equation 1;  $P_{cl} = 53.854 W$ , and  $E_{on}$ ,  $E_{off}$  are 0.124W and

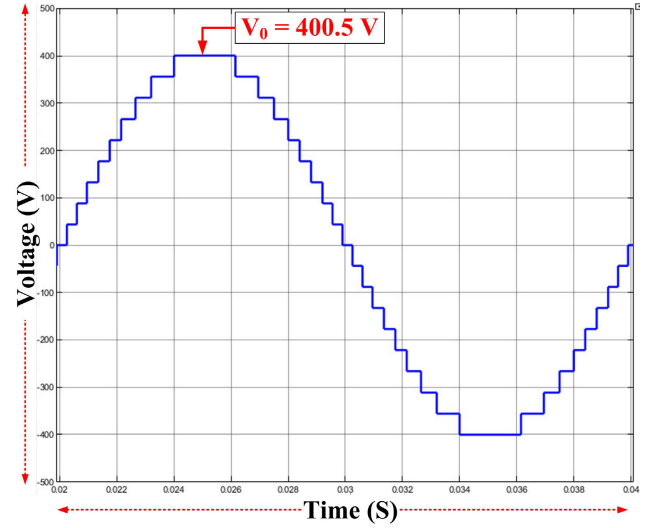


FIGURE 25. Simulation Phase Leg-A output waveform of 19 MLI.

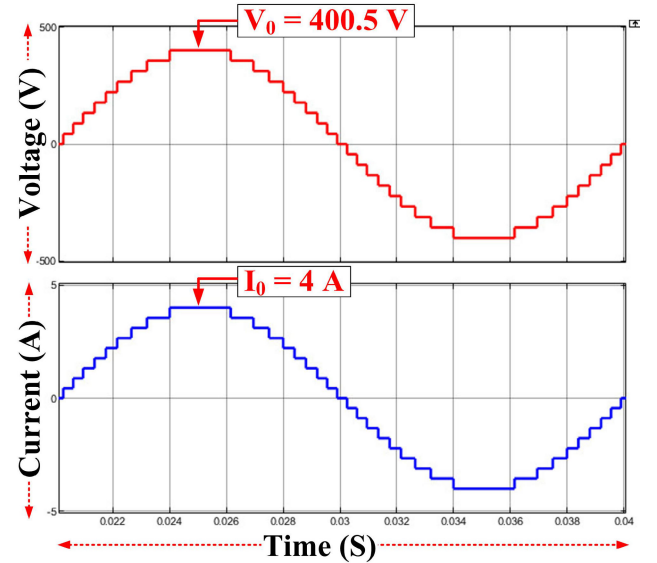


FIGURE 26. Simulation Phase Leg-A output voltage &amp; current waveform of 19 MLI.

0.1625W respectively, from equation 7 the switching losses are 0.2865 W, therefore, the total losses are calculated during the conduction time and switching time by using equation 8 is 54.14W, finally from equation 9 efficiency is 93.67%.

#### IV. COMPARISON WITH RECENT INVERTERS

The proposed inverter contrasted with related topologies of new inverters. Table.2 and Fig.28 to Fig.34 provides a comparison of different component parameters such as several electrical power switches (NSW), several DC sources (NDCS), driver circuits (NDC), clamping diodes (NCMP), clamping capacitors (NCP), efficiency(Eff), TSV, THD and higher output voltage levels required for the inverter proposed. thirteen power switches and three DC sources were used in this topology. Next, the sum of gate driver circuits is thus the same as the number of switches. Then, compared



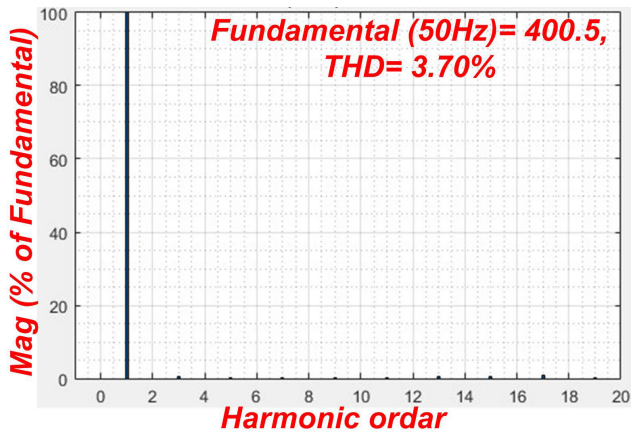


FIGURE 27. Simulation THD of 19 MLI.

TABLE 2. Comparison of proposed with existing MLIs.

Components	[43]	[44]	[45]	[46]	[47]	[48]	Proposed MLI
Switches	12	10	22	11	10	11	13
Sources	1	2	8	5	2	4	3
levels	19	19	19	19	19	19	19
Driver Circuits	11	19	22	19	10	11	13
Clamping Diodes	11	16	26	19	14	11	13
Clamping Capacitors	-	4	-	-	-	-	-
Transformers	3	-	-	-	2	-	-
%THD	-	-	3.72	3.78	3.93	-	3.89
Efficiency (%)	87.725	-	93.49	-	-	-	93.67
TSV (V)	68Vdc	80Vdc	74Vdc	72Vdc	62Vdc	52Vdc	60Vdc

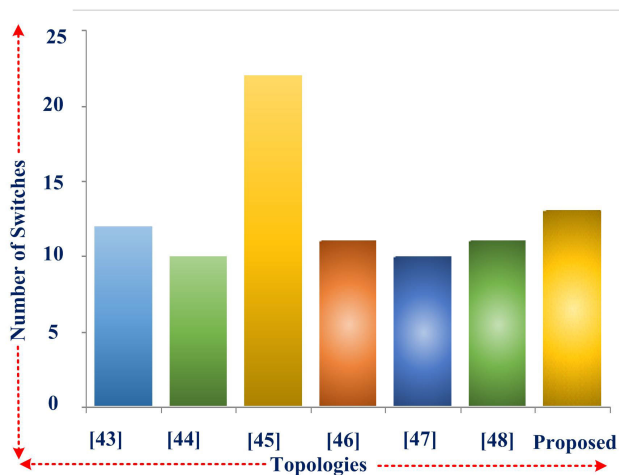


FIGURE 28. Comparison of Recent Inverters vs Proposed MLI with NWS(No. of Switches).

to existing topologies, the suggested asymmetrical topology, each part was calculated for a similar voltage level. While all current topologies will need 10 to 22 switches [43]–[48] and 1 to 8 DC sources to provide an output voltage of 19 rates, the proposed topology needs only 13 switches and three sources with low THD. Compared with traditional topology, the drastically reduced need for switches in the proposed topology to produce better results makes it more suitable

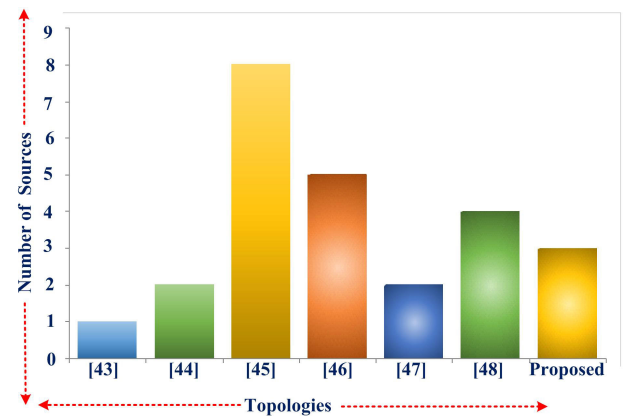


FIGURE 29. Comparison of Recent Inverters vs Proposed MLI with NDSC(No. of Sources).

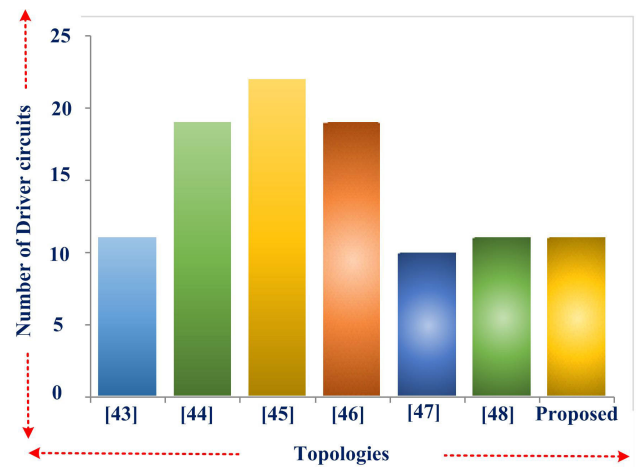


FIGURE 30. Comparison of Recent Inverters vs Proposed MLI with NDC(No. of Drivers Circuits).

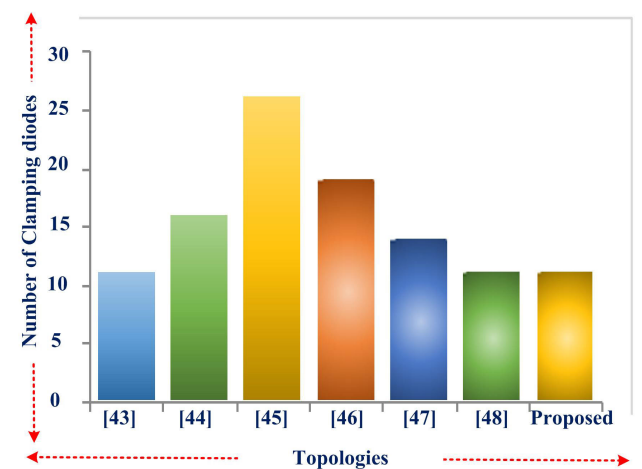


FIGURE 31. Comparison of Recent Inverters vs Proposed MLI with NCMP(No. of Clamping diodes).

for a potential renewable application. Since the DC-link condensers are not required for the proposed topology, they are free from the question of voltage balance. Besides that,



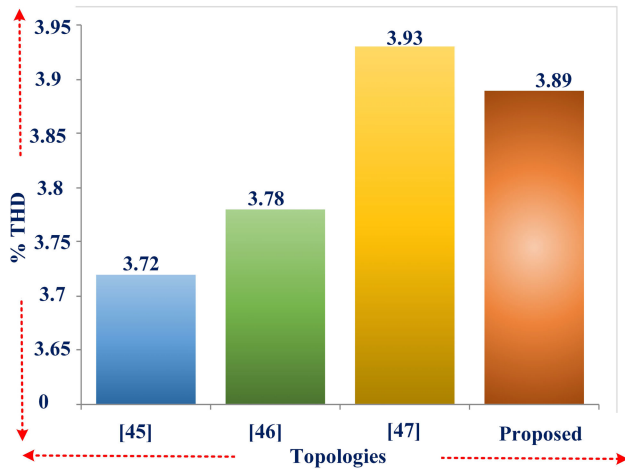


FIGURE 32. Comparison of Recent Inverters vs Proposed MLI with THD.

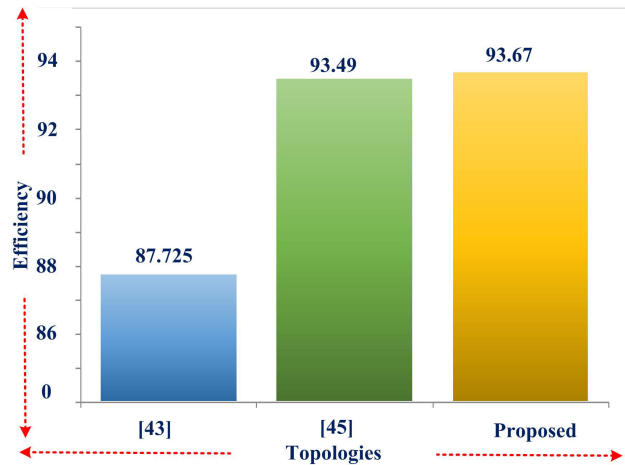


FIGURE 33. Comparison of Recent Inverters vs Proposed MLI with EFF.

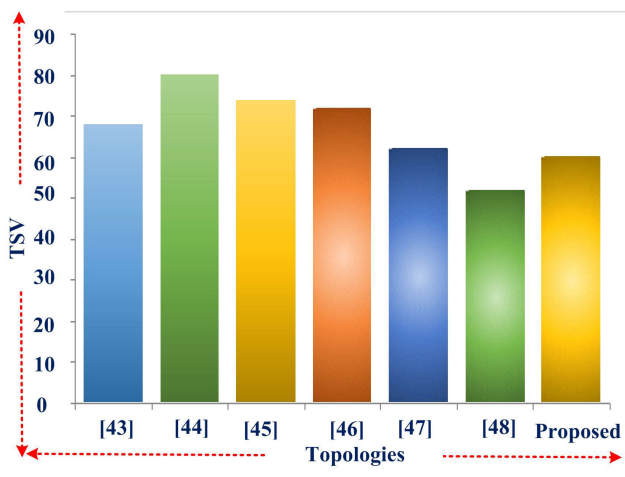


FIGURE 34. Comparison of Recent Inverters vs Proposed MLI with TSV(Total Standing Voltage).

it doesn't require any capacitor clamping and diodes clamping. Every topology, therefore, has its own merits and demerits. The topology suggested has several benefits, such as

fewer switching devices, DC source count and driver circuits, and a minimum number of switches per voltage point. For asymmetric topology, the value of 3.89 percent total harmonic distortion (THD) follows the IEEE 519 requirement. Therefore, it concluded that the proposed topology requires a minimum switch count using both high and fundamental switching frequencies, thus minimizing power losses and costs.

## V. TSV (TOTAL STANDING VOLTAGE) CALCULATION

The maximum voltage stress across all switches is the important parameter for the topology, and it can be represented as the total standing voltage (TSV), which is equal to the sum of maximum voltage stress across the switches [49], [50]. This is an important factor for the selection of switches. Total standing voltage (TSV) is the term which is determined regarding the blocking voltages across all the switches with all voltage levels considered. The voltage stresses across each pair of the complementary switch will be same. However, the TSV is calculated for the proposed topology and is compared with various topologies and found to be the best in having the less standing voltage because of which the losses get decreased. As the blocking voltage capability is less, the rating of the switches is fewer results in cost effective. The voltage stress of the switches in different units is given as: The bidirectional switch voltages are  $V_{Sbi}=V_i$  and the unidirectional switch voltages are  $V_{Suni}=2V_i$  where is  $i=1,2,\dots,n$  and  $n$  is the number of complementary switches. With tertiary mode, the maximum output voltage ( $V_{o,max}$ ) of the proposed topology is:

$$V_{o,max} = 400V \quad (11)$$

The total standing voltage (TSV) is an important factor for the selection of switches. TSV is the addition of the maximum blocking voltage across each semiconductor device [22]. The look-up table for 19-level inverter is shown In Table.3. Therefore, the voltage across the switches are:

$$V_{S1} = 6V_{dc}$$

$$V_{S2} = V_{S5} = 10V_{dc}$$

$$V_{S3} = V_{S4} = 8V_{dc}$$

$$V_{TA} = V_{TC} = 9V_{dc}$$

$$V_{TB} = V_{TD} = 10V_{dc}$$

The voltage stress of unidirectional switches of a bidirectional switch is given as:  $V_{SA}=6V_{dc}$  and  $V_{SB}=2V_{dc}$  As two unidirectional switches are used for the two bidirectional switches, blocks the voltage of  $8V_{dc}$ . Therefore,

$$T_{SV} = 2(V_{S1} + V_{TD} + V_{TB}) + V_{SA} + V_{SB} = 52V_{dc} + 8V_{dc} = 60V_{dc} \quad (12)$$

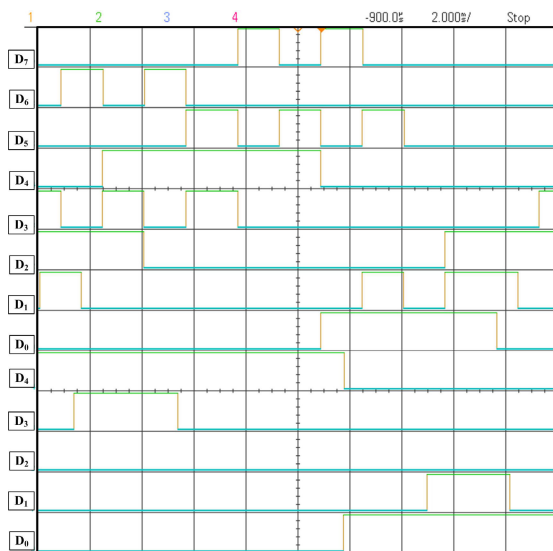
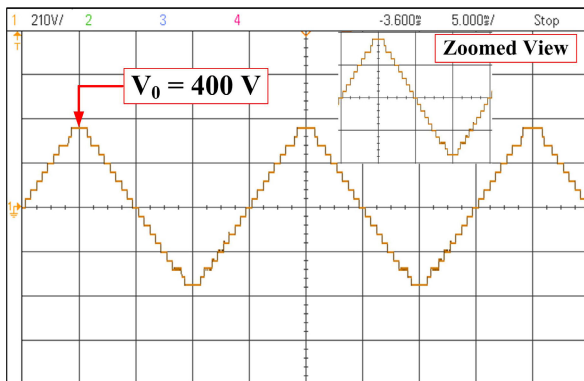
The TSV (total standing voltages) of the proposed inverter is compared with existing inverters is shown in Fig.34.

## VI. EXPERIMENTAL RESULTS

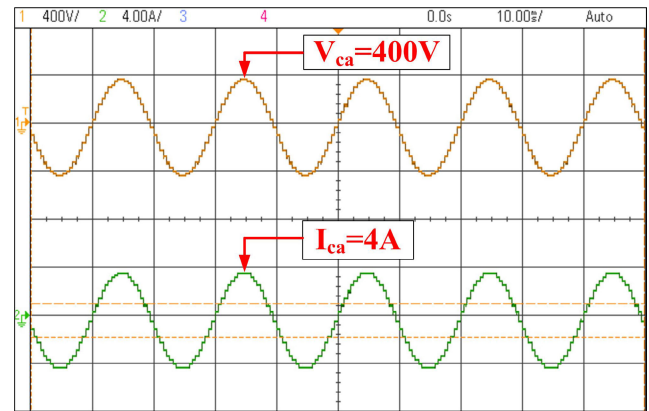
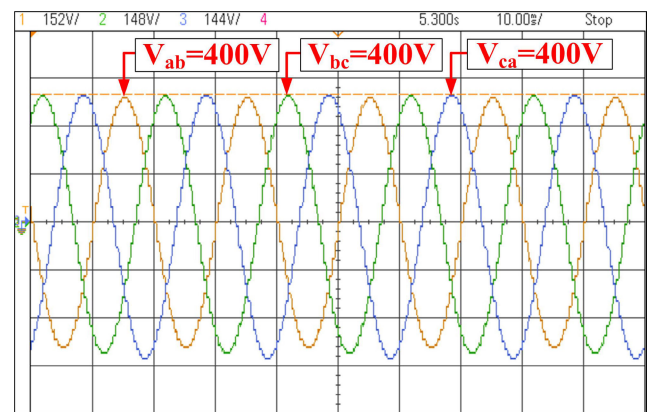
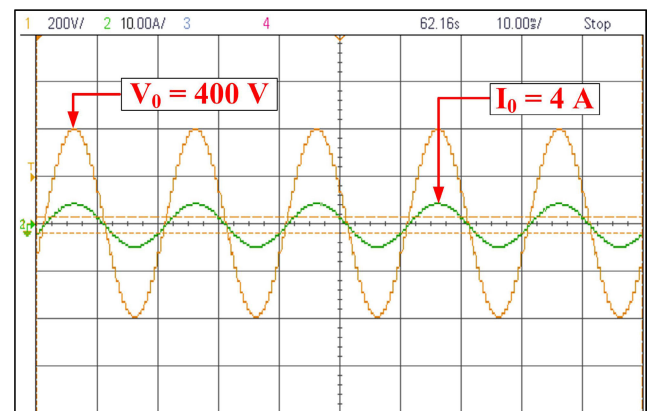
The prototype for 19 level inverter hardware setup systems is recognized and confirmed it experimentally. Fig. 44 specifies the prototype of the multilevel inverter proposed for

**TABLE 3.** The look up table for 19-level inverter.

Level	ON Switches
1	$S_3, S_5, S_A, T_A, T_B$
2	$S_2, S_5, S_A, T_A, T_B$
3	$S_2, S_A, S_B, T_A, T_B$
4	$S_1, S_3, S_5, T_A, T_B$
5	$S_1, S_2, S_5, T_A, T_B$
6	$S_3, S_4, S_A, T_A, T_B$
7	$S_2, S_4, S_A, T_A, T_B$
8	$S_2, S_4, S_5, S_A, S_B, T_A, T_B$
9	$S_1, S_3, S_4, T_B, T_D$
10	$T_A, T_B,$
11	$S_1, S_3, S_4, T_C, T_D$
12	$S_2, S_4, S_5, S_A, S_B, T_C, T_D$
13	$S_2, S_4, S_A, T_C, T_D$
14	$S_3, S_4, S_A, T_C, T_D$
15	$S_1, S_2, S_5, T_C, T_D$
16	$S_1, S_2, S_3, T_C, T_D$
17	$S_2, S_A, S_B, T_C, T_D$
18	$S_2, S_5, S_A, T_C, T_D$
19	$S_3, S_5, S_A, T_C, T_D$

**FIGURE 35.** Experimental Gates Pulses of 19 MLI.**FIGURE 36.** Experimental Output waveform of Phase Leg-A 19 MLI.

this. Simulink block sets are dumped in to the digital I/O ports by dSPACE RTI 1104, and the MATLAB-Simulink is used to implementing the PWM form of staircase modulation (for gate pulses). Use 20 output pins, which are calculated

**FIGURE 37.** Experimental Output voltage & current waveform of 19 MLI.**FIGURE 38.** Experimental Output waveform of Three-Phase 19 MLI.**FIGURE 39.** Experimental Output waveform of Phase Leg-A with R Load.

using physical I/O ports, and real-time interfacing applications are facilitated. The pulse is created from the TLP 250 instrument, which is mined to input the RTI 1104 dSPACE. Gate driver is used to boosting the 5 V to 15 V PWM pulse setup. The control switch is turned on with a 15V pulse. The specifications of the prototype model part are shown in Table 5, the results of the prototype investigation are verified at a steady-state, load disturbance situations are conducted with the help of resistive, inductive loads, and THD is shown in Figures 35 to 43, respectively.

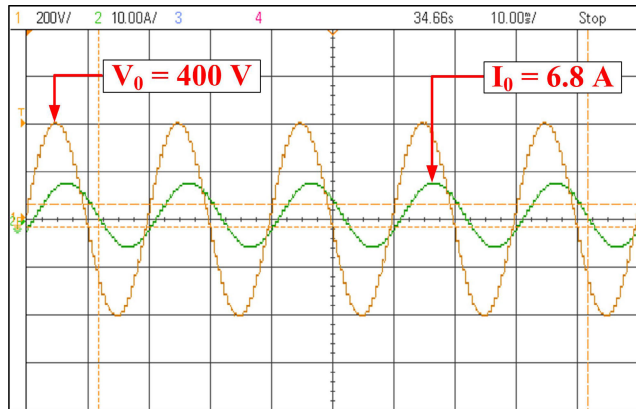


**FIGURE 40.** Experimental Output waveform of Phase Leg-A with L(Motor) Load.

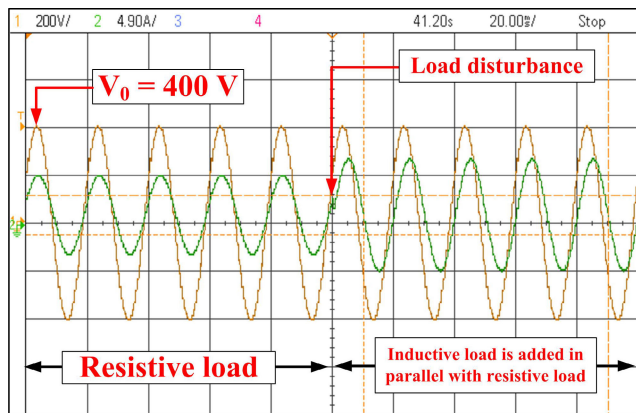


**FIGURE 41.** Experimental Output waveform of Phase Leg-A with RL Load.

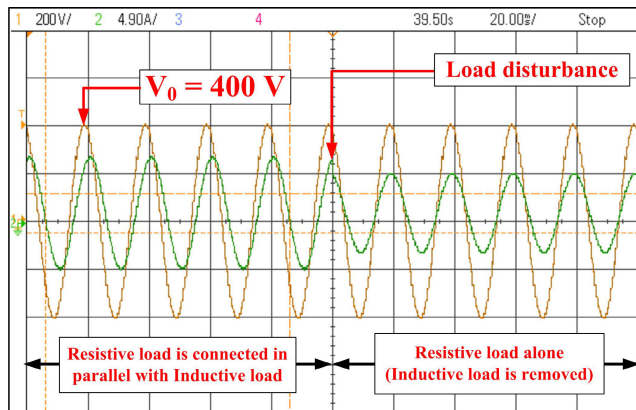


**FIGURE 42.** Experimental Output waveform of Phase Leg-A with LR Load.

The pulses from the gate produced using Driver Circuit TLP250 is shown in Figure.35. The steady-state study was verified with 400 V resistive load (R load), with 4 A attaining output current. The RMS output and voltage found at 282.84 V and 2.828 A current, respectively. The hardware tests are shown respectively in Figure.36, Figure.37, Figure.38 and Figure.39. The experimental prototype results show notably that with 19 output voltage levels. Speciously, the waveform shows that the angle of the transition between the charge current and the charge voltage is zero.

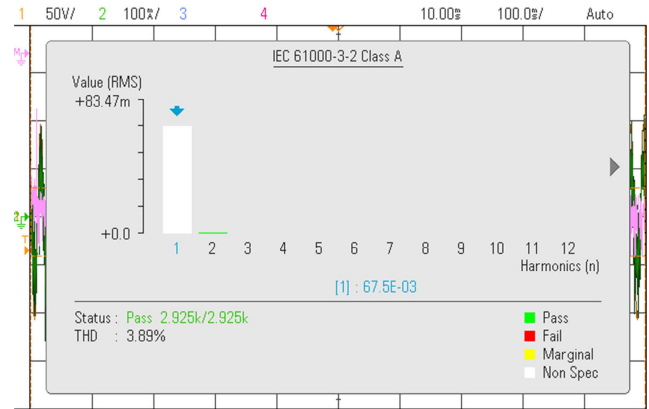


**FIGURE 43.** Experimental THD of 19MLI.

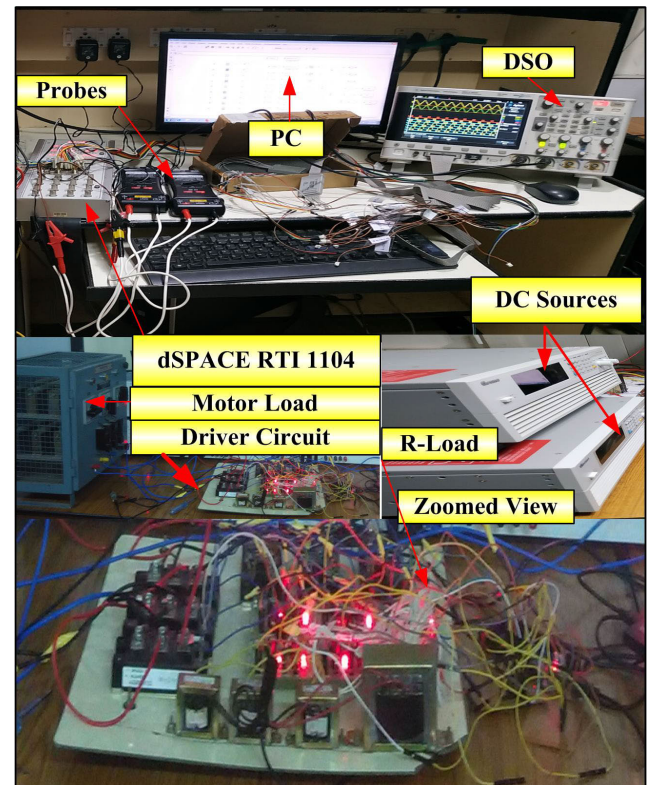


**FIGURE 44.** Prototype Model of 19MLI.

After the achievements of steady-state testing with resistive load, we presented 400 V motor (inductive value is 98mH with 50ohm internal resistance) load (loading power factor) and 6.8 A current. The output current and voltage RMS value are respectively reached with 282.84 V and current 4.808 A. The experimental findings are given in Figure.40. The results show that, with 19 output voltage levels. The phase angle between the lagging charge current and the lagging load voltage is shown in the waveform. To be sure, tons rarely happen distinctly. These can happen continuously in resistive and inductive loads. Typically, where a resistive load is present, an unforeseen addition of inductive load is likely to match the resistive load in parallel or vice versa. The output



**TABLE 4.** Simulation and experimental results.

19 MLI output parameters	Simulation	Experimental
Three phase line to line output voltage	400.5V per phase	400V per phase
Phase leg-A (Line to Line)	400.5V, 4A	400V, 4A
Phase leg-A (Equal magnitude)	400V	400V, 4A
R-Load	400V, 4A	400V, 4A
RMS Voltage and Current	282.4V, 2.828A	282.4V, 2.828A
L-Load (Motor)	400V	400V, 6.8A
THD %	3.7%	3.89%

**TABLE 5.** Experimental specification.

Component	Type	ratings
Switches	IGBT-CM75DU-12H	600V,75A
Driver ICs	TLP250	-
Power supply	Programmable DC Sources	0-500V
Controller	dSPACE	RTI1104
Load	Resistive and Motor (Inductor)	100 ohm and 98mH

voltage must stay steady even in these circumstances is shown in Figure.41 and Figure.42. Figure 39, and Figure 40 shows the experimental voltage THD is 3.89 percent. The experimental component requirements are tabled in Table.5. The proposed MLI could produce higher voltage outputs with fewer hardware components and low THD. The proposed 19 MLI is tested experimentally with L (motor), RL and LR loads. The results got are like simulation. The three-phase line to line voltage of simulation is 400.5 V whereas 400V got experimentally in all phases shown in Table.4. The phase leg-A with equal magnitude are 400V, 4A in both simulation and experimental results. The output waveform of phase leg-A is tested with R, motor, RL and LR loads: with R load, 400V, 4A and 798.62W are got at output, with L (motor) load, 400V and 6.8A are got, In RL load, 400V remains in both resistive and inductive operation resembling the systems output is stable, during load disturbance R and L are in parallel. In LR load, 400V remains in both inductive and resistive operation resembling the stable output, and during the load disturbance, resistive load is alone in the system. THD in simulation is 3.7% whereas 3.89% experimentally. The proposed inverter is designed with optimal hardware components with improved efficiency, reduced power losses, lower THD compared to existing MLIs. The proposed inverter well suits for renewable energy applications.

## VII. CONCLUSION

A three-phase nineteen level asymmetric MLI is tested and implemented. The proposed inverter generates an increased number of output voltage levels with a lesser amount of DC sources and power switches. This inverter makes a voltage at 3.89 % THD, and efficiency is 93.67% got according to IEEE standards. The proposed inverter is tested with study-sate and dynamic load disturbance. In this article, a reduced part count of 19-level inverter topology proposed for high-reliability renewable energy applications. The proposed topology used the inherent properties of sinusoidal voltages to minimize part count to improve the efficiency of the inverter without

the sizing of the circuit components. The proposed inverter balanced well during complex charging (load disturbance) conditions. This inverter is highly adaptive for high-power and renewable energy systems.

## REFERENCES

- [1] A. Nabae, I. Takahashi, and H. Akagi, "A new Neutral-Point-Clamped PWM inverter," *IEEE Trans. Ind. Appl.*, vol. IA-17, no. 5, pp. 518–523, Sep. 1981.
- [2] J. Rodriguez, J.-S. Lai, and F. Zheng Peng, "Multilevel inverters: A survey of topologies, controls, and applications," *IEEE Trans. Ind. Electron.*, vol. 49, no. 4, pp. 724–738, Aug. 2002.
- [3] Y. S. Lai and F. S. Shyu, "Topology for hybrid multilevel inverter," *IEE Proc.-Electr. Power Appl.*, vol. 149, no. 6, pp. 449–458, Nov. 2002.
- [4] T. A. Meynard and H. Foch, "Multi-level choppers for high voltage applications," *EPE J.*, vol. 2, no. 1, pp. 45–50, Jan. 1992.
- [5] O. M. Mueller and J. N. Park, "Quasi-linear IGBT inverter topologies," in *Proc. IEEE Appl. Power Electron. Conf. Expo.*, Feb. 1994, pp. 253–259.
- [6] M. D. Manjrekar, P. K. Steimer, and T. A. Lipo, "Hybrid multilevel power conversion system: A competitive solution for high-power applications," *IEEE Trans. Ind. Appl.*, vol. 36, no. 3, pp. 834–841, May/Jun. 2000.
- [7] R. H. Baker, "High-voltage converter circuit," U.S. Patent 4 203 151, pp. 123–151, May 13, 1980.
- [8] M. E. Ahmed and S. Mekhilef, "Design and implementation of a multi level three-phase inverter with less switches and low output voltage distortion," *J. Power Electron.*, vol. 9, no. 4, pp. 593–603, 2009.
- [9] M. Fracchia, T. Ghiara, M. Marchesoni, and M. Mazzucchelli, "Optimized modulation techniques for the generalized N-level converter," in *Proc. 23rd Annu. IEEE Power Electron. Spec. Conf.*, Jun./Jul. 1992, pp. 1205–1213.
- [10] T. A. Meynard and H. Foch, "Multi-level conversion: High voltage choppers and voltage-source inverters," in *Proc. Rec. 23rd Annu. IEEE Power Electron. Spec. Conf.*, Jun./Jul. 1992, pp. 397–403.
- [11] R. Marquardt, "A new modular voltage source inverter topology," in *Proc. Conf. Rec. EPE*, 2003, doi: [10.1109/PTC.2003.1304403](https://doi.org/10.1109/PTC.2003.1304403).
- [12] A. Lesnicar and R. Marquardt, "An innovative modular multilevel converter topology suitable for a wide power range," in *Proc. IEEE Bologna Power Tech Conf.*, vol. 3, Jun. 2003, p. 6.
- [13] X. Yuan and I. Barbi, "Fundamentals of a new diode clamping multilevel inverter," *IEEE Trans. Power Electron.*, vol. 15, no. 4, pp. 711–718, Jul. 2000.
- [14] M. N. A. Kadir, S. Mekhilef, and H. W. Ping, "Dual vector control strategy for a three-stage hybrid cascaded multilevel inverter," *J. Power Electron.*, vol. 10, no. 2, pp. 155–164, Mar. 2010.
- [15] J. Huang and K. A. Corzine, "Extended operation of flying capacitor multilevel inverters," *IEEE Trans. Power Electron.*, vol. 21, no. 1, pp. 140–147, Jan. 2006.
- [16] C. Feng, J. Liang, and V. G. Agelidis, "Modified phase-shifted PWM control for flying capacitor multilevel converters," *IEEE Trans. Power Electron.*, vol. 22, no. 1, pp. 178–185, Jan. 2007.
- [17] M. R. Banaei, R. Alizadeh, H. Khounjahan, E. Salary, and A. R. Dehghanzadeh, "Z-source-based multilevel inverter with reduction of switches," *IET Power Electron.*, vol. 5, no. 3, pp. 385–392, Mar. 2012.
- [18] M. F. Kangarlu, E. Babaei, and S. Laali, "Symmetric multilevel inverter with reduced components based on non-insulated DC voltage sources," *IET Power Electron.*, vol. 5, no. 5, pp. 571–581, 2012.
- [19] E. Babaei, "A cascade multilevel converter topology with reduced number of switches," *IEEE Trans. Power Electron.*, vol. 23, no. 6, pp. 2657–2664, Nov. 2008.
- [20] G. Waltrich and I. Barbi, "Three-phase cascaded multilevel inverter using power cells with two inverter legs in series," in *Proc. IEEE Energy Convers. Congr. Expo.*, Sep. 2009, pp. 3085–3092.
- [21] J. Dixon and L. Moran, "High-level multistep inverter optimization using a minimum number of power transistors," *IEEE Trans. Power Electron.*, vol. 21, no. 2, pp. 330–337, Mar. 2006.
- [22] M. D. Siddique, S. Mekhilef, N. M. Shah, A. Sarwar, A. Iqbal, and M. A. Memon, "A new multilevel inverter topology with reduce switch count," *IEEE Access*, vol. 7, pp. 58584–58594, 2019, doi: [10.1109/ACCESS.2019.2914430](https://doi.org/10.1109/ACCESS.2019.2914430).

- [23] A. Rufer, M. Veenstra, and K. Gopakumar, "Asymmetric multilevel converter for high resolution voltage phasor generation," in *Proc. EPE*, 1999, p. 10.
- [24] M. Veenstra and A. Rufer, "Control of a hybrid asymmetric multilevel inverter for competitive medium-voltage industrial drives," *IEEE Trans. Ind. Appl.*, vol. 41, no. 2, pp. 655–664, Mar. 2005.
- [25] S. Mekhilef, A. M. Omar, and N. A. Rahim, "Modelling of three-phase uniform symmetrical sampling digital PWM for power converter," in *Proc. Can. Conf. Electr. Comput. Eng.*, May 2008, pp. 1505–1508.
- [26] S. Mariethoz and A. Rufer, "Design and control of asymmetrical multilevel inverters," in *Proc. IEEE 28th Annu. Conf. Ind. Electron. Soc.*, Nov. 2002, pp. 840–845.
- [27] F. Blaabjerg, Z. Chen, and S. B. Kjaer, "Power electronics as efficient interface in dispersed power generation systems," *IEEE Trans. Power Electron.*, vol. 19, no. 5, pp. 1184–1194, Sep. 2004.
- [28] M. V. Rajkumar and P. S. Manoharan, "Modeling and simulation of five-level five-phase voltage source inverter for photovoltaic systems," *J. Przegląd Elektrotechniczny*, vol. 10, no. 10, pp. 237–241, 2013.
- [29] S. Selvakumar, A. Vinothkumar, and M. Vigneshkumar, "An efficient new hybrid cascaded H-bridge inverter for photovoltaic system," in *Proc. 2nd Int. Conf. Devices, Circuits Syst. (ICDCS)*, Mar. 2014, pp. 1–6.
- [30] E. Babaei and S. Laali, "New extendable 15-level basic unit for multilevel inverters," *J. Circuits, Syst. Comput.*, vol. 25, no. 12, Dec. 2016, Art. no. 1650151.
- [31] R. A. Ahmed, S. Mekhilef, and H. Wooi Ping, "New multilevel inverter topology with minimum number of switches," in *Proc. TENCON-IEEE Region 10th Conf.*, Nov. 2010, pp. 1862–1867.
- [32] L. Vijayaraja, S. G. Kumar, and M. Rivera, "A new topology of multilevel inverter with reduced part count," in *Proc. IEEE Int. Conf. Automat./23rd Congr. Chilean Assoc. Autom. Control (ICA-ACCA)*, Oct. 2018, pp. 1–5.
- [33] M. S. A. Dahidah, G. S. Konstantinou, and V. G. Agelidis, "SHE-PWM control for asymmetrical hybrid multilevel flying capacitor and H-bridge converter," in *Proc. IEEE 9th Int. Conf. Power Electron. Drive Syst.*, Dec. 2011, pp. 29–34.
- [34] E. Babaei, "Charge balance control methods for a class of fundamental frequency modulated asymmetric cascaded multilevel inverters," *J. Power Electron.*, vol. 11, no. 6, pp. 811–818, Nov. 2011.
- [35] E. Bircenas, S. Ramirez, V. Cardenas, and R. Echavarria, "Cascade multilevel inverter with only one DC source," in *Proc. 8th IEEE Int. Power Electron. Congr. Tech. Proc. CIEP*, Oct. 2002, pp. 171–176.
- [36] M. Sabahi, A. R. Marami Iranqa, K. M. Bahrani, K. M. Bahrani, and M. B. B. Sharifian, "Harmonics elimination in a multilevel inverter with unequal DC sources using genetic algorithm," in *Proc. Int. Conf. Electr. Mach. Syst.*, Aug. 2011, pp. 1–5.
- [37] B.-R. Lin, T.-C. Wei, and H.-K. Chiang, "An eight-switch three-phase VSI for power factor regulated shunt active filter," *Electr. Power Syst. Res.*, vol. 68, no. 2, pp. 157–165, Feb. 2004.
- [38] A. Nami, F. Zare, A. Ghosh, and F. Blaabjerg, "A hybrid cascade converter topology with series-connected symmetrical and asymmetrical diode-clamped H-bridge cells," *IEEE Trans. Power Electron.*, vol. 26, no. 1, pp. 51–65, Jan. 2011.
- [39] C. Dhanamjayulu and S. Meikandasivam, "Implementation and comparison of symmetric and asymmetric multilevel inverters for dynamic loads," *IEEE Access*, vol. 6, pp. 738–746, 2018.
- [40] C. Dhanamjayulu and S. Meikandasivam, "Design and implementation of symmetric cascaded multilevel inverter using sub multi-cells," *J. Adv. Res. Dyn. Control Syst.*, vol. 9, no. 18, pp. 1657–1668, 2017.
- [41] C. Dhanamjayulu, G. Arunkumar, B. J. Pandian, C. V. R. Kumar, M. P. Kumar, A. R. A. Jerin, and P. Venugopal, "Real-time implementation of a 31-level asymmetrical cascaded multilevel inverter for dynamic loads," *IEEE Access*, vol. 7, pp. 51254–51266, 2019.
- [42] C. Dhanamjayulu, G. Arunkumar, B. Jaganatha Pandian, and S. Padmanaban, "Design and implementation of a novel asymmetrical multilevel inverter optimal hardware components," *Int. Trans. Electr. Energy Syst.*, vol. 30, no. 2, pp. 1–28, Feb. 2020.
- [43] F. Kang, "A modified cascade transformer-based multilevel inverter and its efficient switching function," *Electr. Power Syst. Res.*, vol. 79, no. 12, pp. 1648–1654, 2009.
- [44] R. Barzegarkhoo, E. Zamiri, M. Moradzadeh, and H. Shadabi, "Symmetric hybridised design for a novel step-up 19-level inverter," *IET Power Electron.*, vol. 10, no. 11, pp. 1377–1391, Sep. 2017.
- [45] K.-M. Tsang and W.-L. Chan, "Single DC source three-phase multilevel inverter using reduced number of switches," *IET Power Electron.*, vol. 7, no. 4, pp. 775–783, Apr. 2014.
- [46] R. S. Alishah, D. Nazarpour, M. Sabahi, and S. H. Hosseini, "New hybrid structure for multilevel inverter with fewer number of components for high-voltage levels," *IET Power Electron.*, vol. 7, no. 1, pp. 96–104, Jan. 2014.
- [47] J. Venkataramanaiah, Y. Suresh, and A. K. Panda, "Design and development of a novel 19-level inverter using an effective fundamental switching strategy," *IEEE J. Emerg. Sel. Topics Power Electron.*, vol. 6, no. 4, pp. 1903–1911, Dec. 2018.
- [48] E. Babaei, A. Dehqan, and M. Sabahi, "A new topology for multilevel inverter considering its optimal structures," *Electr. Power Syst. Res.*, vol. 103, pp. 145–156, Oct. 2013.
- [49] M. D. Siddique, A. Iqbal, M. A. Memon, and S. Mekhilef, "A new configurable topology for multilevel inverter with reduced switching components," *IEEE Access*, vol. 8, pp. 188726–188741, 2020.
- [50] M. D. Siddique, S. Mekhilef, N. M. Shah, J. S. M. Ali, M. Seyedmahmoudian, B. Horan, and A. Stojcevski, "Switched-capacitor-based boost multilevel inverter topology with higher voltage gain," *IET Power Electron.*, vol. 13, no. 14, pp. 3209–3212, Nov. 2020.



**C. DHANAMJAYULU** (Member, IEEE) received the B.Tech. degree in electronics and communication engineering from JNTU University, Hyderabad, India, the M.Tech. degree in control and instrumentation systems from IIT Madras, Chennai, India, and the Ph.D. degree in power electronics from the Vellore Institute of Technology, Vellore, India. He is currently a Postdoctoral Researcher with the Department of Energy Technology, Aalborg University, Esbjerg, Denmark.

Since 2010, he has been a Senior Assistant Professor with the Vellore Institute of Technology, where he is currently a Faculty Member and a member of the Department of Control and Automation, School of Electrical Engineering, Vellore Institute of Technology, and also a Senior Assistant Professor. He was invited as a Visiting Researcher with the Department of Energy Technology, Aalborg University, funded by the Danida Mobility Grant, Ministry of Foreign Affairs of Denmark, on Denmark's International Development Cooperation. His research interests include multilevel inverters, power converters, active power filters, power quality, grid-connected systems, smart grid, electric vehicle, electric spring, and tuning of memory elements and controller parameters using soft-switching techniques for power converters, average modeling, steady-state modeling, and small-signal modeling stability analysis of the converters and inverters.



**PALANISAMY KALIANNAN** (Senior Member, IEEE) received the bachelor's degree in electrical engineering from the KSR College of Technology, India, in 2000, the master's degree (Hons.) in applied electronics from the Coimbatore Institute of Technology, India, in 2004, and the Ph.D. degree in electrical engineering from the Vellore Institute of Technology, Vellore, India, in 2013. He has been a Deputy Director of Electrical Maintenance and Projects and an Associate Professor of

the Energy and Power Electronics Division, Vellore Institute of Technology, where he has been the Head of the Center for Smart Grid Technology since 2007. From 2016 to 2018, he was the Head of the Department of Energy and Power Electronics Division. He has authored over 96 scientific articles in referred conference proceedings and international journals in the field of renewable energy, battery energy storage, multilevel converters, and power quality. He is a certified Energy Auditor by the Bureau of Energy Efficiency, Government of India. He has taken up various consultancy projects in energy efficiency and power quality improvement.





**SANJEEVIKUMAR PADMANABAN** (Senior Member, IEEE) received the bachelor's degree in electrical engineering from the University of Madras, Chennai, India, in 2002, the master's degree (Hons.) in electrical engineering from Pondicherry University, Puducherry, India, in 2006, and the Ph.D. degree in electrical engineering from the University of Bologna, Bologna, Italy, in 2012. He was an Associate Professor with Vellore Institute of Technology from 2012 to

2013. In 2013, he joined the National Institute of Technology, India, as a Faculty Member. In 2014, he was invited as a Visiting Researcher with the Department of Electrical Engineering, Qatar University, Doha, Qatar, funded by the Qatar National Research Foundation, Government of Qatar. He continued his research activities with the Dublin Institute of Technology, Dublin, Ireland, in 2014. He served as an Associate Professor with the Department of Electrical and Electronics Engineering, University of Johannesburg, Johannesburg, South Africa, from 2016 to 2018. Since 2018, he has been a Faculty Member with the Department of Energy Technology, Aalborg University, Esbjerg, Denmark. He has authored over 300 scientific articles.

He is a Fellow of the Institution of Engineers, India, the Institution of Electronics and Telecommunication Engineers, India, and the Institution of Engineering and Technology, U.K. He was a recipient of the Best Paper cum Most Excellence Research Paper Award from the IET-SEISCON'13, IET-CEAT'16, IEEE-EECSI'19, and IEEE-CENCON'19, and five best paper awards from ETAEERE'16 and sponsored lecture notes in *Electrical Engineering*, Springer book. He is an Editor/Associate Editor/Editorial Board for refereed journals, including the IEEE SYSTEMS JOURNAL, the IEEE TRANSACTION ON INDUSTRY APPLICATIONS, IEEE ACCESS, *IET Power Electronics*, *IET Electronics Letters*, and the *Wiley-International Transactions on Electrical Energy Systems*, a Subject Editorial Board Member of *Energy Sources Energies Journal*, *MDPI*, and the Subject Editor of the *IET Renewable Power Generation*, *IET Generation, Transmission and Distribution*, and *FACTS journal* (Canada).



**PANDAV KIRAN MAROTI** (Member, IEEE) received the bachelor's degree in electronics and telecommunication from Dr. Babasaheb Ambedkar Marathwada University, Aurangabad, India, in 2011, the M.Tech. degree (Hons.) in power electronics and drives from the Vellore Institute of Technology, Vellore, India, in 2014. He is currently pursuing the Ph.D. degree in the field of power electronics with the University of Johannesburg, South Africa. He was an Assistant Professor

with the Marathwada Institute of Technology, Aurangabad, India, from 2014 to 2016. He is currently a Visiting Researcher with Qatar University. He received the Global Experience Scholarship for his Ph.D. study. He has authored or coauthored scientific articles in the field of power electronics (multilevel dc/dc and dc/ac converter and multiphase open winding inverter). He is an Active Professional Member of the Industrial Electronics, Power Electronics, Industrial Application, and Young Professionals societies. He is also an Active Reviewer Member of various reputed international conferences and journal, including the IEEE and the IET. He received the Best Paper Award from ETAEERE in 2016 sponsored lecture note in *Electrical Engineering*, Springer book series.



**JENS BO HOLM-NIELSEN** (Senior Member, IEEE) was born in 1954. He received the Ph.D. degree. He is currently the Head of the Research Group of Bioenergy and Green Engineering, Department of Energy Technology, Aalborg University, Denmark. He has experience in the field of biomass feedstock production, biorefinery concepts, and biogas production, for 30 years. He was a Board Member of research and development committees of the cross-governmental body of

biogas developments in Denmark from 1993 to 2009. He is a Secretary and/or the Chair of NGO biogas and bioenergy organizations. He is the Chair and a Presenter of sustainable and 100 percent renewables and SDG-17 goals. He has experience of a variety of EU projects. He was an organizer of international conferences, workshops, and training programs in EU, USA, Canada, China, Brazil, India, Iran, Russia, Ukraine, among others. His research interests include managing research, development, and demonstration programs in integrated agriculture, environment and energy systems. He has fulfilled the biomass and bio-energy research and development projects. His principal focuses on biofuels, biogas, and biomass resources. He is an EDU and supervises M.Sc. and Ph.D. students in these research fields. He has involved in training programs, such as international courses, training programs, and supervision for Ph.D. students, and academic staff, governmental bodies, and experts in bioenergy systems. His full biography at [www.aau.dk](http://www.aau.dk) profile search Jens Bo Holm-Nielsen.

...